PAPER

# Study of anisotropy of convective optical underwater turbulence and the effect of the mean water temperature in the presence of a varying temperature gradient on it

IOP Publishing | Astro Ltd Laser Physics
Laser Phys. **32** (2022) 095602 (9pp) https://doi.org/10.1088/1555-6611/ac8bd2

# Study of anisotropy of convective optical underwater turbulence and the effect of the mean water temperature in the presence of a varying temperature gradient on it

**Ebrahim Mohammadi Razi**[1,*], **Reza Shokoohi**[1] and **Saifollah Rasouli**[2,3,4]

[1] Faculty of Physics, Department of Basic Sciences, University of Bojnord, 1339 Bojnord, Iran
[2] Department of Physics, Institute for Advanced Studies in Basic Sciences (IASBS), 45137-66731 Zanjan, Iran
[3] Optics Research Center, Institute for Advanced Studies in Basic Sciences (IASBS), 45137-66731 Zanjan, Iran
[4] The Abdus Salam ICTP, Strada Costiera 11, Trieste 34151, Italy

E-mail: e.mohammadi@ub.ac.ir

Received 3 August 2022
Accepted for publication 14 August 2022
Published 7 September 2022

**Abstract**

In this paper, the anisotropy of optical convective underwater turbulence is investigated in terms of the variance of angle of arrival (AOA) fluctuations of a narrow laser beam propagating through it in different sections of the medium. The collimated laser beam with a wavelength 532 nm and a diameter 1 cm, which passes through a convective underwater turbulence. The turbulence is generated in a water tank with dimensions of 20 cm $\times$ 36 cm $\times$ 20 cm, which is installed on a flat surface electrical heater. During the experiments, the mean water temperature (MWT) can be changed from room temperature to 34 °C by increasing the heater temperature. The use of the heater also generates a temperature gradient in the medium. The laser beam propagates along a horizontal path with a length of 20 cm inside the tank at different altitudes from the heater source, as well as at different distances from one of the side walls of the turbulent medium. After passing the laser beam through the turbulent medium, the fluctuations of the AOA components in the vertical and horizontal directions are measured. From the time series of the measured AOA fluctuations, their variances are determined. The anisotropy of the medium is investigated by comparing the variance of AOA components measured in the vertical and horizontal directions. We show that the variances of both of vertical and horizontal components of the AOA fluctuations are increased with the MWT, and they are saturated at higher MWTs. In addition, different anisotropic behaviors are observed for the variances of the measured AOA fluctuations at the vicinity of the lateral wall and upper surface of the water. At the vicinity of the lateral wall the variances of the AOA fluctuations in the horizontal component are larger, but at the vicinity of the upper surface the variances of the AOA fluctuations in the vertical component are dominant. This behavior may be caused by the change of the convection motion direction in the turbulent fluid.

* Author to whom any correspondence should be addressed.

 

Keywords: anisotropic turbulence, angle of arrival, Rayleigh–Bénard convection, underwater turbulence

(Some figures may appear in colour only in the online journal)

## 1. Introduction

In recent years, underwater turbulence has attracted the attention of researchers in the field of military and sciences owing to its various applications [1]. A variety of applications such as underwater imaging [2–4], underwater optical wireless communications [5–8], remote sensing [9, 10] and military uses, have made laser beam propagation through underwater turbulence one of the most attractive topics. The propagation of a laser beam through such a medium is limited by some phenomena including absorption, scattering, and optical turbulence. The temperature fluctuations and salinity are two main origins of the optical underwater turbulence [1]. Unlike atmospheric turbulence, in addition to the temperature and salinity fluctuations, their average values also affect the light signal propagation through underwater turbulence [11]. Thermal convection turbulence is a common process in nature. Rayleigh–Bénard convection is a simplest paradigm system to study a turbulent thermal convection. In this system, a fluid layer is heated from below and cooled from above. However in some studies the turbulent medium is only heated from below [12–20]. The effects of convective turbulence have been studied on the propagation of a light beam through convective air turbulence [12–20] and underwater [21–28]. Bissonnette [21] and Gurvich *et al* [22] were among the pioneers in the studying of the optical properties of underwater convective turbulence. Bissonnette by calculating the refractive index structure constant as well as the structure function of refractive index fluctuations showed that the artificial convective turbulence obeys the Kolmogorov model. He also revealed that the statistical properties of the medium is similar to atmospheric turbulence. In addition, the strength of underwater-created turbulence was approximately 200 times stronger than the strength of the atmospheric turbulence. Elliott *et al* [23] created a convective turbulence in a scattering cell by maintaining an unstable temperature gradient in the ethanol and investigated the spatial spectrum of the temperature fluctuations as well as the structure function of refractive index fluctuations. They also studied the turbulence strength versus the heater power that used for heating the liquid. Maccioni and Dainty [24] by the use of a Shack–Hartmann sensor, analyzed the angle of arrival (AOA) correlations of a wavefront that has propagated through a convective turbulent water cell. Computing the mean variance of the AOA fluctuations in single column and single row, they studied isotropy and homogeneity of the turbulence medium. Results showed that the turbulence is homogeneous but anisotropic. The reason of anisotropy was cited by the existence of temperature gradients in the medium. The fluctuations of the AOA (indirectly with the Fried parameter) were studied as a function of the temperature difference between the heated and cooled plates in [25, 26]. An argument about the volume of effective isotropy is also presented. The propagation of a laser beam through Rayleigh–Bénard turbulence was investigated experimentally and by a numerical simulation method in [27], and using centroid motion of the beam, the refractive index structure constant, $C_n^2$, was determined. In addition, the strength of the convective underwater turbulence and its effects on the image degradation and velocity vector maps were investigated in [28].

Various models are proposed to describe atmospheric turbulence based on the turbulence homogeneity and isotropy, and have been generalized to study the underwater one. Many studies have shown that the atmospheric turbulence [19, 29–31] as well as the underwater [32, 33] are anisotropic. Recently, many papers have been published about the effects of anisotropic underwater turbulence on the optical communication systems [34–48].

As can be concluded from the above-reviewed articles, the effects of anisotropic underwater turbulence on the beam propagation have been frequently investigated. However, based on our knowledge, the source of anisotropy and anisotropy behavior in different regions of underwater convective turbulence have not been studied. It is worth mentioning that in [23–26] characteristics of turbulence have been investigated in a small section of medium. In this work, in the presence of a varying temperature gradient a convective underwater turbulence with different mean water temperatures (MWTs) was generated, and for different MWTs, the variances of two components of AOA in different sections of turbulent medium were investigated.

In addition, we report observation of different anisotropic behaviors for the variances of the measured AOA fluctuations at the vicinity of the lateral wall and upper surface of the turbulent water.

## 2. Experiment

Figure 1(a) shows a schematic diagram of the experimental setup used in this work. As is seen a narrow beam laser with a Gaussian intensity profile and a wavelength 532 nm passes through a telescopic system to be a collimated wave with a diameter 1 cm, then propagates through an underwater turbulent medium. The underwater turbulent medium consists of a water tank with dimensions of 20 cm $\times$ 20 cm $\times$ 36 cm where the laser beam propagates along the tank side having a length 20 cm. The water tank is placed on an electrical heater with adjustable temperature. This system evokes a Rayleigh–Bénard convection. The beam path altitude from the heater surface can be easily adjusted using a jack installed under the heater. The MWT increases as the heater temperature rises. After passing through the turbulent medium, the laser beam is focused on a charge-coupled device (CCD) camera using a positive lens having a focal length 2.5 cm. The position of

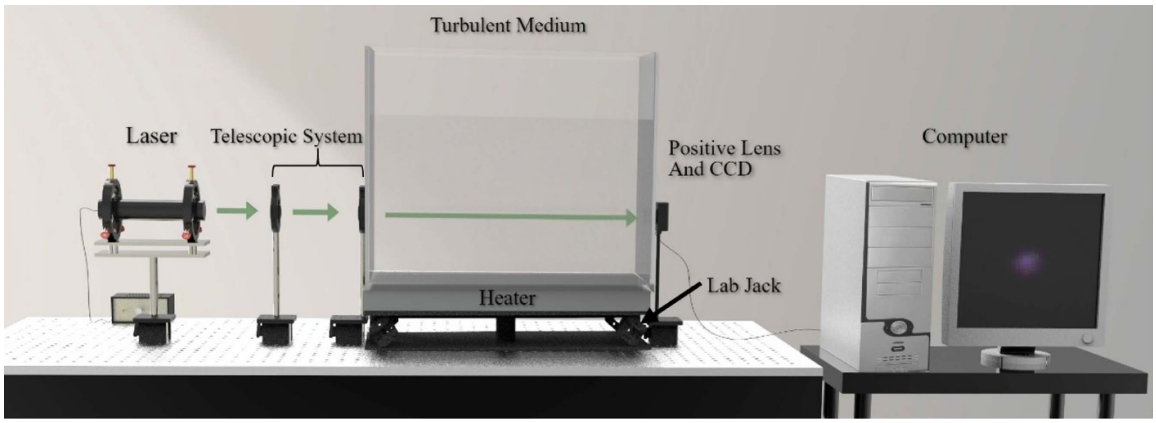


(a)

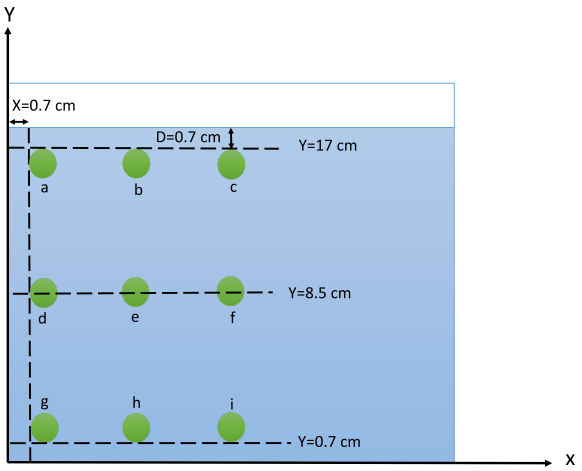


(b)

**Figure 1.** (a) Schematic diagram of the experimental set up, (b) cross section of water tank and paths used the laser beam propagation through the underwater turbulence.

the focus point of the light beam on the CCD camera depends on the beam AOA. The AOA components fluctuate due to the optical turbulence. The temperature fluctuations are the main origin of the optical turbulence in a convective underwater turbulence. The frame rate of image recording and exposure time are set to 600 frame per second and 0.3 ms, respectively. The MWT of the medium can be varied from 19 °C to 34 °C with a step size of 0.5 °C with an accuracy 0.1 °C. To study the effect of dominant direction of the fluid motion on the AOA fluctuations, as well as the underwater turbulence anisotropy, the light beam propagates through the medium at different distances from the bottom, Y, and side walls, X, of the water tank. Figure 1(b) shows the water tank cross section as well as the locations where the light beam propagates through the medium in different experiments. In locations denoted by a, b and c, the distance of the beam path from the water surface is 0.7 cm, also in h, i and g locations, the distance of the beam path from the bottom of tank equals to 0.7 cm, and the distance of the beam path from the right wall of the tank in a, d, and e locations is also equal. As mentioned, the water salinity in all experiments is considered zero and the optical turbulence is caused by the temperature fluctuations. At the end of the beam path, the AOA of the light beam is measured in two directions perpendicular to the propagation's direction denoting by $x$ and $y$. Finally, the variance of these fluctuations is calculated in the two directions from 20 000 recorded frames for each experiment. Each experiment with a given path of the beam inside the tank (illustrated by a to i letters in figure 1(b)) was performed in one day. To cancel out the unwanted vibrations, the whole arrangement is placed on a pneumatic optical table.

## 3. Results and discussion

Details of determining and calculation of AOA components have been previously described in [19, 29]. In brief, the $x$-component of AOA is determined from the displacement of the laser beam focal spot as follows:

$$\alpha_{xi} = \frac{l_x(x_{gi} - \bar{x}_{gi})}{f}, \tag{1}$$

where $l_x$ is pixel size in $x$-direction on the image plane, $x_{gi}$ and $\bar{x}_{gi}$ are, $x$-coordinates of the image center and it is mean position and $f$ denotes the focal length of the positive lens. The $y$-component of AOA is calculated with the same way. The image center or centroid is defined as the center of intensity gravity and determined by the wavefront gradients averaged over the spot image. Its $x$-component is calculated by

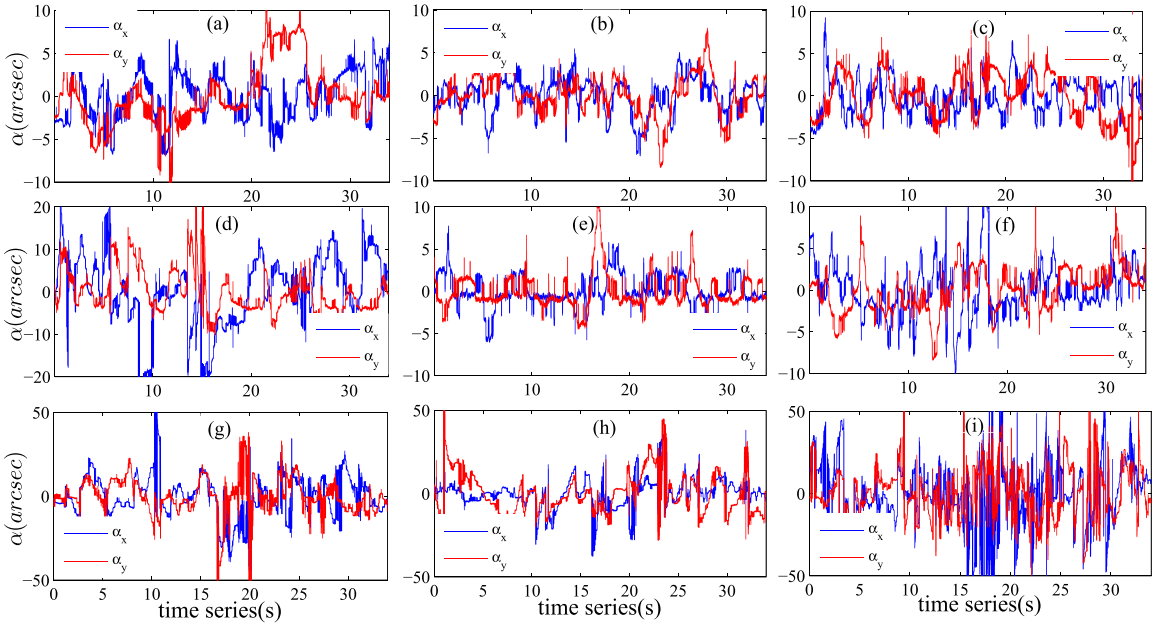


**Figure 2.** Time series of AOA fluctuations in $x$- and $y$-direction for different paths of the beam in underwater turbulence shown in figure 1(b) at the MWT of 34 °C.

$$x_g = I_{tot}^{-1} \int\int xI(x,y)dxdy, \tag{2}$$

where $I_{tot}$ is the total flux and $I(x,y)$ is the light intensity distribution on the spot image at the focal plane of the convex lens.

To study the effects of MWTs on the AOA fluctuations, two components of AOA in two directions perpendicular to the propagation direction are determined for different MWTs. Figure 2 shows the time series of AOA fluctuations of the light beam in two directions at different MWTs and different paths of the beam in the turbulent medium. As is seen, in both directions, the amplitude of the AOA fluctuations increases as the distance from the bottom of the water tank decreases. The variance of the AOA fluctuations in $x$ and $y$ directions is calculated from the displacements of image centroids. According to equation (1) the variance of AOA in $x$ direction can be written as

$$\sigma_{\alpha_x}^2 = \frac{l_x^2}{f^2}\sigma_x^2, \tag{3}$$

where $\sigma_{\alpha_x}^2$ and $\sigma_x^2$ are the variance of AOA fluctuations and variance of centroid fluctuations. The uncertainty or error in $\sigma_{\alpha_x}^2$ can be found by using the rules of propagation of uncertainty. If the original uncertainties are independed and random, the error of the $\sigma_{\alpha_x}^2$ is calculated from [49]

$$\frac{\delta\sigma_{\alpha_x}^2}{\sigma_{\alpha_x}^2} = \sqrt{\left(\frac{\delta\sigma_x^2}{\sigma_x^2}\right)^2 + \left(\frac{\delta l_x^2}{l_x^2}\right)^2 + \left(\frac{\delta f^2}{f^2}\right)^2}, \tag{4}$$

where $\delta$ shows the measurement error of corresponding parameter. In these measurements $\frac{\delta\sigma_x^2}{\sigma_x^2} = \sqrt{\frac{2}{N-1}}$, and $N$ is the total number of the data set. For $N = 20000$, $\frac{\delta\sigma_x^2}{\sigma_x^2}$ was obtained as 0.01. Considering $\delta l_x$ is negligible and $\delta f = 10^{-4}$ m, $\frac{\delta\sigma_{\alpha_x}^2}{\sigma_{\alpha_x}^2}$ was obtained as 0.03. It should be noted that for all different propagation paths shown in figure 1(b), using the jack, only the location of the water tank was shifted and the relative positions of the beam and the imaging system were fixed during different experiments. Therefore, the error sources such as the focal length of the lens are same in all experiments.

Figure 3 shows the variance of the AOA fluctuations in $x$ and $y$ directions as function of the MWT in the locations shown in figure 1(b). As is seen the dependence of the AOA fluctuations variance on MWT in each direction exhibits two different trends: increasing and saturated behaviors. Since, the value of AOA variance is proportional to the intensity of the turbulence, therefore the turbulence intensity differs in two regions. The variance of AOA fluctuations in the first region with the MWTs of less than 24 °C, increases with the MWT while for the MWTs of more than 24 °C, it is saturated. The index of refraction structure constant, $C_n^2$, for Gaussian beam can be calculated from variance of AOA fluctuations by [50]

$$\sigma_\alpha^2 \cong 1.093 C_n^2 L D^{-1/3}\left[a + 0.618\Lambda^{11/6}\left(\frac{kD^2}{L}\right)^{-1/3}\right], \quad \times (L/k)^{1/2} \ll D, \tag{5}$$

where $L$, $D$ and $k$ are the propagation length, lens diameter, and optical wave number, respectively, and $a = \frac{1-\Theta^{8/3}}{1-\Theta}$ and $\Theta = 1 + \frac{L}{F}$, where $F$ denotes the receiver plane phase front radius of curvature. Figure 4 shows the calculated $C_n^2$ as function of the MWT in the locations shown in figure 1(b). The results of the simulation in [27] confirm the similar incremental and saturation behavior of $C_n^2$ with the temperature gradient between hot and cold plates.

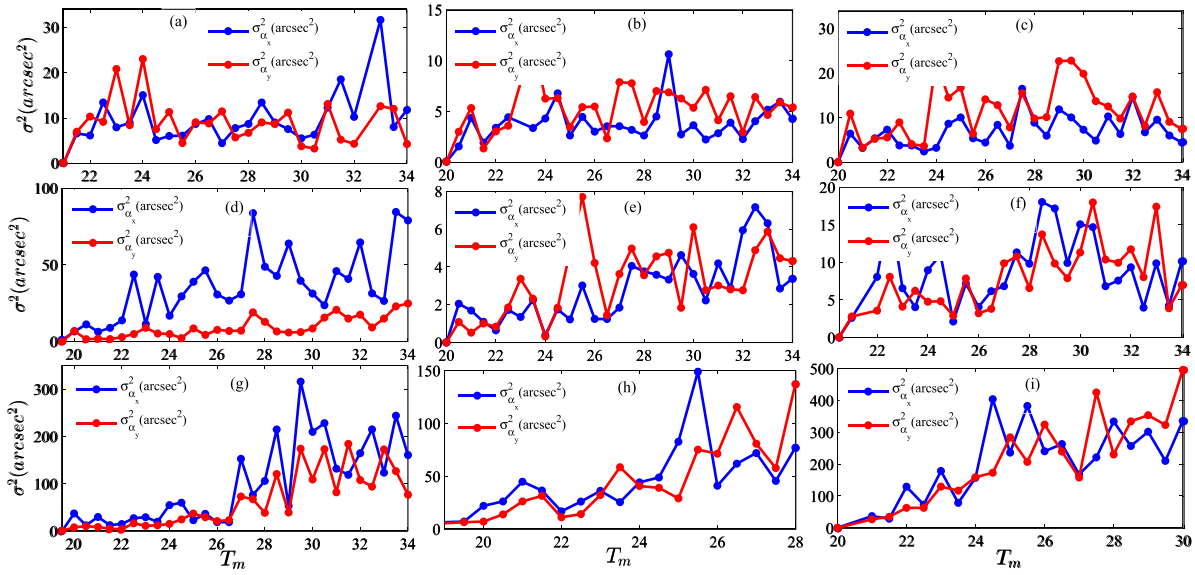


**Figure 3.** Variance of the AOA fluctuations in $x$ and $y$ direction versus MWT for different paths of the beam in the underwater turbulence shown in figure 1(b).

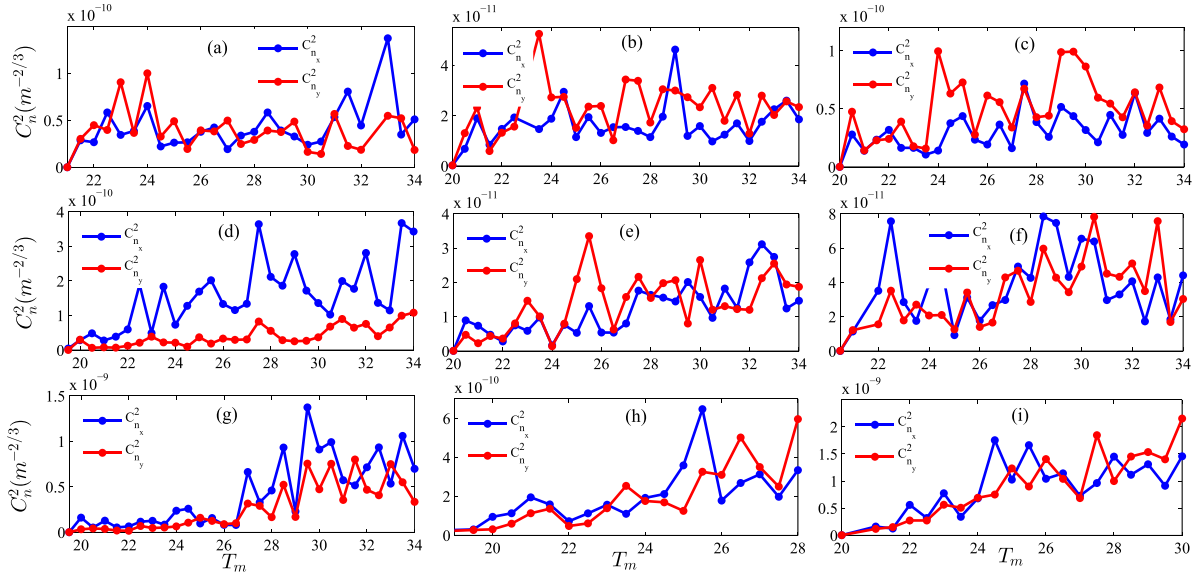


**Figure 4.** The index of refraction structure constant, $C_n^2$, versus MWT for different paths of the beam in the underwater turbulence shown in figure 1(b).

In the literature, underwater turbulence is divided into weak, strong and saturated cases in terms of its intensity [1]. In this research, with increasing the MWT, strong and saturated turbulence is produced. The turbulence intensity is more for the paths are closer to the heat source and thus in paths g, h and i in figure 1(b), the measured variance values and related $C_n^2$ are greater than the other paths. Contrary to [21–28], in the current work, there is no a cold water chamber above the tank. In the first glance, this might limit the experimentation time under constant conditions. To investigate this issue, the total data collection time was divided into two equal time intervals. Each time interval contains 10 000 frames. The AOA variances for the first and second time intervals were plotted versus the MWT in figures 5 and 6, respectively. By comparing the results shown in the figures we see that they show a similar behavior. This means that, the experiment condition was approximately constant during the experimentation time.

Concerning figure 3, another feature is the anisotropy of the convective underwater turbulence. As it is seen, the variance of the AOA fluctuations are not equal in two directions at most MWT and locations. In other words, convective underwater turbulence is an anisotropic one.

For a better visualization of the anisotropy, the difference of the variance of AOA components in two directions, is plotted in figure 7. As it is seen, for all the beam paths shown in figure 1(b), the difference of the variance of AOA components

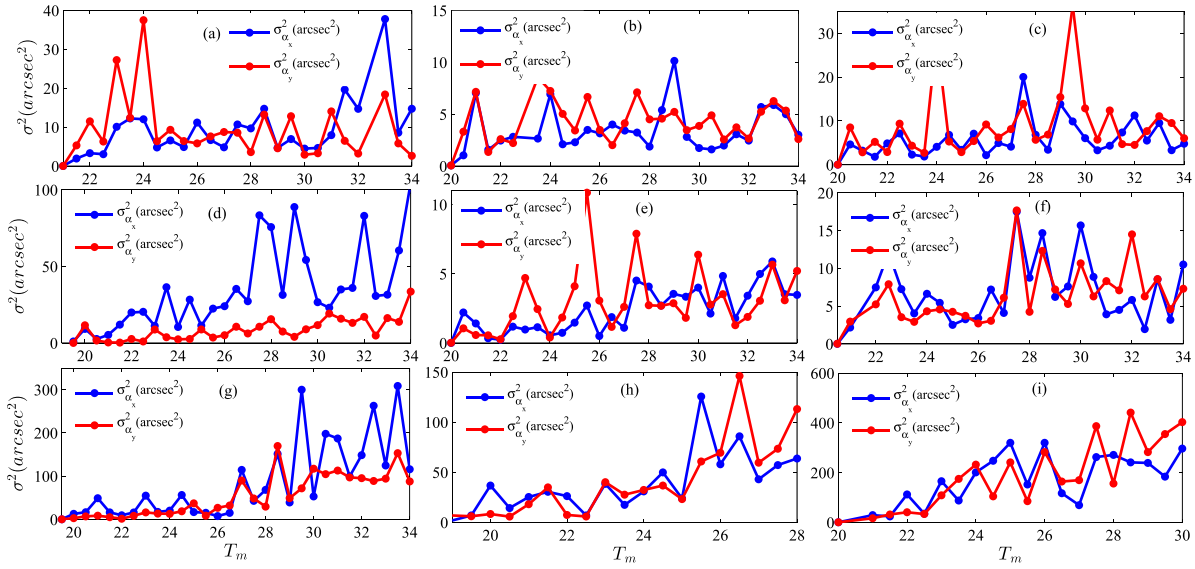


**Figure 5.** Variance of the AOA fluctuations in *x*- and *y*- direction versus MWT for different paths of the beam in the underwater turbulence shown in figure 1(b). Initial 10 000 frames were used to calculate the variance of the AOA fluctuations.

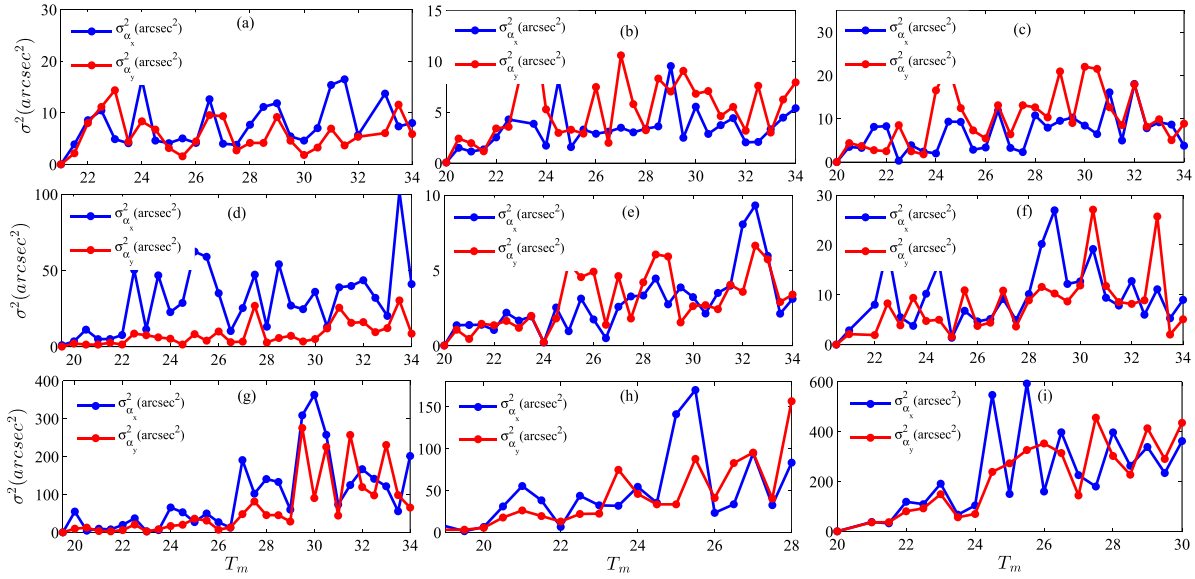


**Figure 6.** Variance of the AOA fluctuations in *x*- and *y*- direction versus MWT for different paths of the beam in the underwater turbulence shown in figure 1(b). final 10 000 frames were used to calculate the variance of the AOA fluctuations.

is not equal to zero. This guarantees anisotropy of the turbulent medium at any location and any MWT. In addition, for two beam paths of b and c where the distance of the light beam path from the water surface is 0.7 cm, the difference of variance of AOA components is positive at most of the MWTs, i.e. for these locations, the anisotropy is positive. The fluid rising from the bottom due to the convection, is expected to move toward the sides of the water tank. Thus in locations b and c, the *x*-component of the fluid velocity is greater than the *y*-component. In other words, predominant direction of motion in these locations is *x*-direction. While in location a, the fluid moves dominantly downwards, i.e. in *y*-direction. For locations d and g, a similar result is achieved. The difference of the *x* and *y* components of the fluid velocity in locations d and g are greater than the location a. Accordingly, in locations d and g, the difference between the variance in the two directions increases with MWT. With this justification, it can be said that at the upper edge of the fluid, $Y = 17$ cm and $X = 9$, 18 cm, the fluid mostly moves in *x*-direction and at $Y = 0.7$, 8.5 cm and $X = 0.7$ cm, the dominant direction of motion is along *y*-direction. This means that the anisotropy can be characterized in the underwater turbulence in the presence of temperature gradient by the fluid motion direction. Figure 8 shows the *y*-component of AOA variance versus its *x*-component at three beam path heights of 0.7, 8.5 and 17 cm. Aforementioned results are better perceived in this figure. As it is seen from figure 8(a), the data of locations b and c are above the line $\sigma_y^2 = \sigma_x^2$, while for locations d ($Y = 8.5$ cm, $X = 0.7$ cm) and

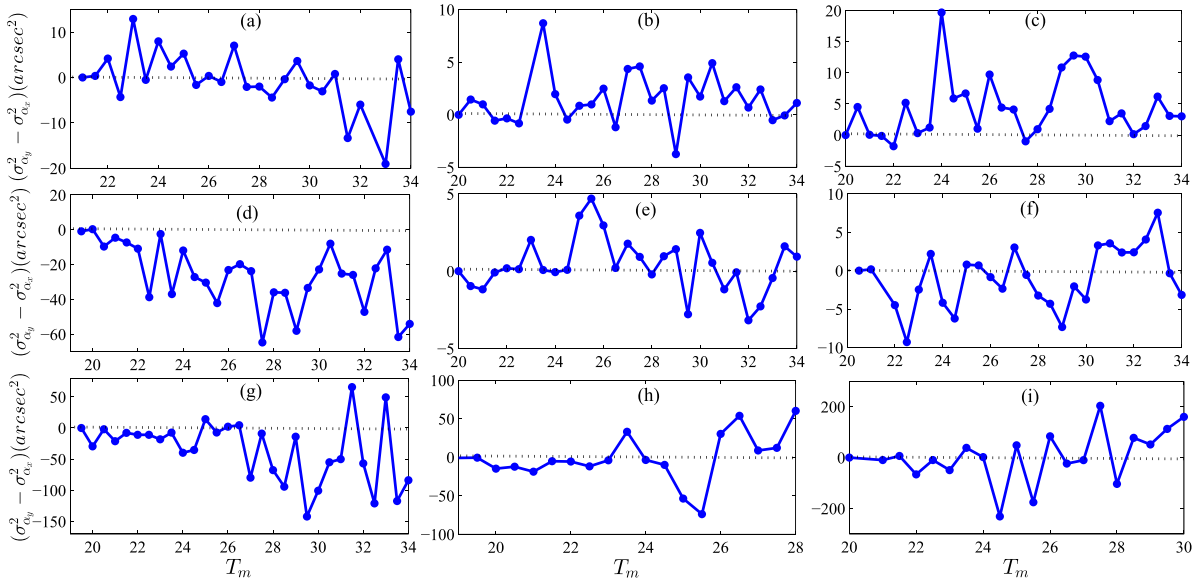


**Figure 7.** Difference of the AOA variances in two directions versus MWT in underwater turbulence for the different beam paths shown in figure 1(b).

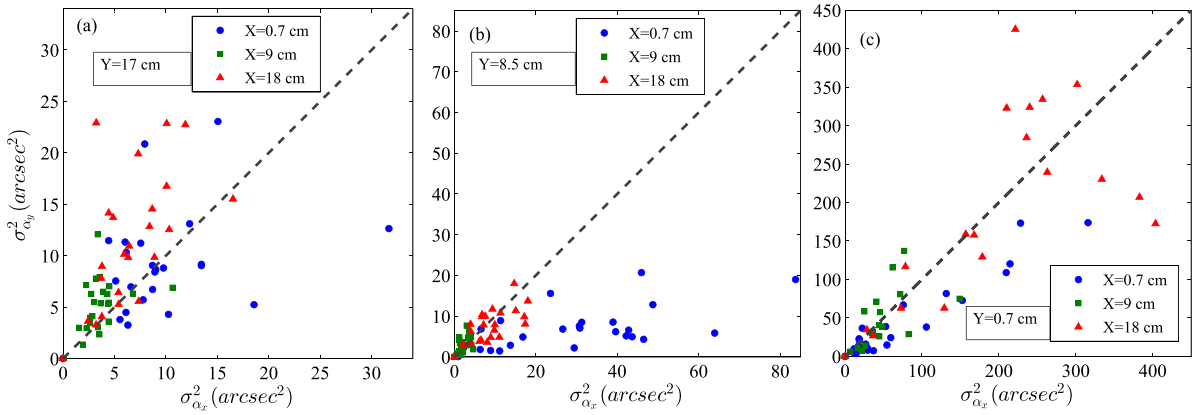


**Figure 8.** $Y$-component of the variances of AOA fluctuations versus its $x$-component at different heights (h) and different distances from the tank wall (d). The dash line is $\sigma_y^2 = \sigma_x^2$.

g ($Y = 0.7$ cm, $X = 0.7$ cm) in figures 8(b) and (c) the data are below it.

As mentioned in the introduction section, Maccioni and Dainty [24] have studied the anisotropy of the convective underwater turbulent but only in a cross-section having an area of $5 \times 5$ mm$^2$. In addition, they have averaged the variance of AOA fluctuations over the horizontal (vertical) rows (columns). This averaging (on the rows/columns) removes some features of the anisotropy behavior. In the current work, we investigated the anisotropy in different parts of the turbulence medium with averaging in a direction.

## 4. Conclusion

In this work, based on the analysis of the variance of AOA fluctuations in two directions perpendicular to the propagation path of the light beam, the anisotropy of convective underwater turbulence and its origin were investigated. The studied convective underwater turbulence was created using an electrical heater under a water filled tank. A light beam with a wavelength of 532 nm and a diameter of 1 cm propagated in different paths in the medium. At the end of the path, the AOA of the light beam in two directions perpendicular to the propagation direction, was measured. The MWT varied from 19 °C to 34 °C and its effect on the variance of AOA fluctuations in different sections of medium were investigated. The results showed that with increasing the MWT, the variance of the AOA fluctuations exhibits two different trends: incremental and saturated behaviors. In addition, by comparison of variances of the components of AOA fluctuations it was founded that the convective underwater turbulence is an anisotropic medium. We also find that the anisotropy behaviors different near the boundary of the fluid with air or side walls of tank in comparing with the other locations. The fluid rising from the bottom due to the convection, is expected to move toward the sides of the water tank. Thus along propagation paths near the liquid-air separation surface, predominant

direction of motion is $x$-direction. While in locations near the side walls of the tank, the fluid moves dominantly downwards, i.e. in $y$-direction. The dominant movement in the $x$-($y$-) direction will cause the variance of $y$-($x$-) component of the AOA fluctuations to dominate. This means that the anisotropy can be characterized in the underwater turbulence in the presence of temperature gradient by the fluid motion direction.

## ORCID iD

Ebrahim Mohammadi Razi https://orcid.org/0000-0002-8250-9980

## References


[1] Korotkova O 2019 Light propagation in a turbulent ocean *Progress in Optics* vol 64 (Amsterdam: Elsevier) pp 1–43

[2] Hou W W 2009 A simple underwater imaging model *Opt. Lett.* **34** 2688–90

[3] Kocak D M, Dalgleish F R, Caimi F M and Schechner Y Y 2008 A focus on recent developments and trends in underwater imaging *Mar. Technol. Soc. J.* **42** 52–67

[4] Jaffe J S 1990 Computer modeling and the design of optimal underwater imaging systems *IEEE J. Ocean. Eng.* **15** 101–11

[5] Yi X, Li Z and Liu Z 2015 Underwater optical communication performance for laser beam propagation through weak oceanic turbulence *Appl. Opt.* **54** 1273–8

[6] Kaushal H and Kaddoum G 2016 Underwater optical wireless communication *IEEE Access* **4** 1518–47

[7] Zeng Z, Fu S, Zhang H, Dong Y and Cheng J 2017 A survey of underwater optical wireless communications *IEEE Commun. Surv. Tutor.* **19** 204–38

[8] Jamali M V, Salehi J A and Akhoundi F 2017 Performance studies of underwater wireless optical communication systems with spatial diversity: MIMO scheme *IEEE Trans. Commun.* **65** 1176–92

[9] Korotkova O 2018 Enhanced backscatter in LIDAR systems with retro-reflectors operating through a turbulent ocean *J. Opt. Soc. Am.* A **35** 1797–804

[10] Korotkova O and Yao J-R 2020 Bi-static lidar systems operating in the presence of oceanic turbulence *Opt. Commun.* **460** 125119

[11] Yao J-R, Zhang H-J, Wang R-N, Cai J-D, Zhang Y and Korotkova O 2019 Wide-range Prandtl/Schmidt number power spectrum of optical turbulence and its application to oceanic light propagation *Opt. Express* **27** 27807–19

[12] Carnevale M, Crosignani B and Di Porto P 1968 Influence of laboratory generated turbulence on phase fluctuations of a laser beam *Appl. Opt.* **7** 1121–3

[13] Fitzjarrald D E 1976 An experimental study of turbulent convection in air *J. Fluid Mech.* **73** 693–719

[14] Consortini A, Fusco G, Rigal F, Agabi A and Sun Y Y 1997 Experimental verification of thin-beam wandering dependence on distance in strong indoor turbulence *Waves Random Media* **7** 521

[15] Bertolotti M, Carnevale M, Crosignani B and Di Porto P 1969 Influence of thermal turbulence in a convective ascending stream on phase fluctuations of a laser beam *Appl. Opt.* **8** 1111–4

[16] Funes G, Gulich D, Zunino L, Pérez D G and Garavaglia M 2007 Behavior of the laser beam wandering variance with the turbulent path length *Opt. Commun.* **272** 476–9

[17] Mohammadi Razi E, Rasouli S, Dashti M and Niemela J J 2021 A high-resolution wavefront sensing method to investigate the annular Zernike polynomials behaviour in the indoor convective air turbulence in the presence of a 2D temperature gradient *J. Mod. Opt.* **68** 994–1001

[18] Mohammadi Razi E and Rasouli S 2019 Impacts of the source temperature and its distance on the statistical behavior of the convective air turbulence *Appl. Phys.* B **125** 1

[19] Razi E M and Rasouli S 2014 Measuring significant inhomogeneity and anisotropy in indoor convective air turbulence in the presence of 2D temperature gradient *J. Opt.* **16** 045705

[20] Gulich D, Funes G, Zunino L, Pérez D G and Garavaglia M 2007 Angle-of-arrival variance's dependence on the aperture size for indoor convective turbulence *Opt. Commun.* **277** 241–6

[21] Bissonnette L R 1977 Atmospheric scintillation of optical and infrared waves: a laboratory simulation *Appl. Opt.* **16** 2242–51

[22] Gurvich A S, Kallistratova M A and Martvel F E 1977 An investigation of strong fluctuations of light intensity in a turbulent medium at a small wave parameter *Radiophys. Quantum Electron.* **20** 705–14

[23] Elliott R A, Kerr J R and Pincus P A 1979 Optical propagation in laboratory-generated turbulence *Appl. Opt.* **18** 3315–23

[24] Maccioni A and Dainty J C 1997 Measurement of thermally induced optical turbulence in a water cell *J. Mod. Opt.* **44** 1111–26

[25] Zhang J and Zeng Z Y 1994 Wavefront tilt power spectral density from image motion induced by laboratory-generated turbulence *Proc. SPIE* **2312** 327–36

[26] Zhang J and Zeng Z 2001 Statistical properties of optical turbulence in a convective tank: experimental results *J. Opt. A: Pure Appl. Opt.* **3** 236

[27] Nootz G, Matt S, Kanaev A, Judd K P and Hou W 2017 Experimental and numerical study of underwater beam propagation in a Rayleigh–Bénard turbulence tank *Appl. Opt.* **56** 6065–72

[28] Matt S, Hou W, Goode W and Hellman S 2017 Introducing SiTTE: a controlled laboratory setting to study the impact of turbulent fluctuations on light propagation in the underwater environment *Opt. Express* **25** 5662–83

[29] Razi E M and Rasouli S 2017 Investigation of inhomogeneity and anisotropy in near ground layers of atmospheric air turbulence using image motion monitoring method *Opt. Commun.* **383** 255–9

[30] Rasouli S, Niry M D, Rajabi Y, Panahi A A and Niemela J J 2014 Applications of 2-D Moiré deflectometry to atmospheric turbulence *J. Appl. Fluid Mech.* **7** 651–7

[31] Gu Y and Gbur G 2010 Scintillation of Airy beam arrays in atmospheric turbulence *Opt. Lett.* **35** 3456–8

[32] Mohammadi Razi E, Behboodi M and Rasouli S 2022 A study on angle of arrival fluctuations in a temperature-, salinity-and sweetness-induced underwater optical turbulence *Waves Random Complex Media* 1–14

[33] Godeferd F S and Staquet C 2003 Statistical modelling and direct numerical simulations of decaying stably stratified turbulence. Part 2. Large-scale and small-scale anisotropy *J. Fluid Mech.* **486** 115–59

[34] Xu G and Lai J 2020 Average capacity analysis of the underwater optical plane wave over anisotropic moderate-to-strong oceanic turbulence channels with the Málaga fading model *Opt. Express* **28** 24056–68

[35] Ata Y and Baykal Y 2018 Effect of anisotropy on bit error rate for an asymmetrical Gaussian beam in a turbulent ocean *Appl. Opt.* **57** 2258–62

[36] Huang X, Deng Z, Shi X, Bai Y and Fu X 2018 Average intensity and beam quality of optical coherence lattices in

oceanic turbulence with anisotropy *Opt. Express* **26** 4786–97
[37] Yang Y, Yu L, Wang Q and Zhang Y 2017 Wander of the short-term spreading filter for partially coherent Gaussian beams through the anisotropic turbulent ocean *Appl. Opt.* **56** 7046–52
[38] Wu Y, Zhang Y, Zhu Y and Hu Z 2016 Spreading and wandering of Gaussian–Schell model laser beams in an anisotropic turbulent ocean *Laser Phys.* **26** 095001
[39] Lu L, Wang Z, Zhang P, Qiao C, Fan C, Zhang J and Ji X 2015 Phase structure function and AOA fluctuations of plane and spherical waves propagating through oceanic turbulence *J. Opt.* **17** 085610
[40] Ata Y 2022 Structure function, coherence length and angle-of-arrival variance for Gaussian beam propagation in turbulent waters *J. Opt. Soc. Am.* A **39** 63–71
[41] Chen M and Zhang Y 2019 Effects of anisotropic oceanic turbulence on the propagation of the OAM mode of a partially coherent modified Bessel correlated vortex beam *Waves Random Complex Media* **29** 694–705
[42] Wang X, Yang Z and Zhao S 2019 Influence of oceanic turbulence on propagation of Airy vortex beam carrying orbital angular momentum *Optik* **176** 49–55
[43] Li Y, Yu L and Zhang Y 2017 Influence of anisotropic turbulence on the orbital angular momentum modes of Hermite-Gaussian vortex beam in the ocean *Opt. Express* **25** 12203–15
[44] Baykal Y 2018 Effect of anisotropy on intensity fluctuations in oceanic turbulence *J. Mod. Opt.* **65** 825–9
[45] Li Y, Zhang Y, Zhu Y and Chen M 2016 Effects of anisotropic turbulence on average polarizability of Gaussian Schell-model quantized beams through ocean link *Appl. Opt.* **55** 5234–9
[46] Hu Z, Liu H, Xia J, He A, Li H, Du Z, Chen T, Li Z and Lü Y 2020 Propagation characteristics of the perfect vortex beam in anisotropic oceanic turbulence *Appl. Opt.* **59** 9956–62
[47] Xu Y, Shi H and Zhang Y 2018 Effects of anisotropic oceanic turbulence on the power of the bandwidth-limited OAM mode of partially coherent modified Bessel correlated vortex beams *J. Opt. Soc. Am.* A **35** 1839–45
[48] Zhu Y, Zhang J, Wang X, Du Y, Yang Y, He F and Kou L 2021 Performance analysis of digital pulse interval modulation for underwater optical communication link in anisotropy oceanic turbulence *Proc. SPIE* **11885** 1188514
[49] Frieden R 2012 *Probability, Statistical Optics and Data Testing: A Problem Solving Approach* (Berlin: Springer)
[50] Andrews L C and Phillips R L 2005 *Laser Beam Propagation Through Random Media* 2nd edn